R Coronae Borealis and dustless hydrogen-deficient carbon stars likely have different oxygen isotope ratios

V. Karambelkar, M. M. Kasliwal, P. Tisserand, G. C. Clayton, C. L. Crawford, S. G. Anand, T. R. Geballe, E. Montiel

A&A 667, A84 (2022)
https://doi.org/10.1051/0004-6361/202142918

Astronomy & Astrophysics

R Coronae Borealis and dustless hydrogen-deficient carbon stars likely have different oxygen isotope ratios⋆

V. Karambelkar[1], M. M. Kasliwal[1], P. Tisserand[2], G. C. Clayton[3], C. L. Crawford[3], S. G. Anand[1], T. R. Geballe[4], and E. Montiel[5]

[1] Cahill Center for Astrophysics, California Institute of Technology, Pasadena, CA 91125, USA
e-mail: viraj@astro.caltech.edu
[2] Sorbonne Universités, UPMC Univ. Paris 6 et CNRS, UMR 7095, Institut d'Astrophysique de Paris, IAP, 75014 Paris, France
[3] Department of Physics & Astronomy, Louisiana State University, Baton Rouge, LA 70803, USA
[4] Gemini Observatory/NSF's NOIRLab, 670 N A'ohoku Pl, Hilo, HI 96720, USA
[5] SOFIA-USRA, NASA Ames Research Center, MS 232-12, Moffett Field, CA 94035, USA

Received 15 December 2021 / Accepted 12 August 2022

ABSTRACT

Context. R Coronae Borealis (RCB) and dustless Hydrogen-deficient Carbon (dLHdC) stars are believed to be remnants of low mass white dwarf mergers. These supergiant stars have peculiar hydrogen-deficient carbon-rich chemistries and stark overabundances of ^{18}O. RCB stars undergo dust formation episodes resulting in large-amplitude photometric variations that are not seen in dLHdC stars. Recently, the sample of known dLHdC stars in the Milky Way has more than quintupled with the discovery of 27 new dLHdC stars.
Aims. It has been suggested that dLHdC stars have lower ^{16}O/^{18}O than RCB stars. We aim to compare the ^{16}O/^{18}O ratios for a large sample of dLHdC and RCB stars to examine this claim.
Methods. We present medium resolution ($R \approx 3000$) near-infrared spectra of 20 newly discovered dLHdC stars. We also present medium resolution ($R \approx 3000-8000$) K-band spectra for 49 RCB stars. Due to the several free parameters and assumptions in our fitting strategy, we provide wide range estimates on the ^{16}O/^{18}O ratios of seven dLHdC and 33 RCB stars that show ^{12}C^{16}O and ^{12}C^{18}O absorption bands, and present the largest sample of such ^{16}O/^{18}O wide-range values for dLHdC and RCB stars to date.
Results. We find that six of the seven dLHdC stars have ^{16}O/^{18}O < 0.5, while 28 of the 33 RCB stars have ^{16}O/^{18}O > 1. We also confirm that unlike RCB stars, dLHdC stars do not show strong blueshifted (>200 km s^{-1}) He I 10 833 Å absorption, suggesting the absence of strong, dust-driven winds around them.
Conclusions. Although we only can place wide range estimates on the ^{16}O/^{18}O and these are more uncertain in cool RCBs, our medium resolution spectra suggest that most dLHdC stars have lower ^{16}O/^{18}O than most RCB stars. This confirms one of the first, long-suspected spectroscopic differences between RCB and dLHdC stars. The different oxygen isotope ratios rule out the existing picture that RCB stars represent an evolved stage of dLHdC stars. Instead, we suggest that whether the white dwarf merger remnant is a dLHdC or RCB star depends on the mass ratios, masses and compositions of the merging white dwarfs. Future high resolution spectroscopic observations will help confirm and more precisely quantify the difference between the oxygen isotope ratios of the two classes.

Key words. stars: AGB and post-AGB – stars: carbon – circumstellar matter – stars: late-type – supergiants – infrared: stars

1. Introduction

R Coronae Borealis (RCB) and dustless Hydrogen-deficient Carbon (dLHdC)[1] stars are supergiants characterized by a peculiar chemical composition – an acute deficiency of hydrogen and an overabundance of carbon (Clayton 1996; Feast 1996; Lambert & Rao 1994). Together, they form the class of Hydrogen-deficient Carbon (HdC) stars. Their chemical compositions suggest that they are remnants of He-core and CO-core white dwarf (WD) mergers (Webbink 1984; Iben & Tutukov 1984; Saio & Jeffery 2002), making them low mass counterparts of type Ia supernovae in the double-degenerate (DD) scenario (Fryer et al. 2008). In addition to peculiar chemical compositions, RCB stars experience rapid photometric declines (up to 8 mag in V band) that are attributed to dust formation episodes (Clayton 2012). dLHdC stars do not show any such declines or any significant infrared (IR) excess, suggesting that they do not undergo any dust formation (Warner 1967; Goswami et al. 2010; Tisserand 2012). Why RCB stars produce dust while dLHdC stars do not, despite having no other known chemical differences is still a mystery.

It has been relatively easier to identify RCB stars than dLHdC stars owing to their spectacular photometric variations. There are 128 RCB stars known in the Milky Way, while only five Galactic dLHdC stars had been known for the last four decades (Clayton 2012; Tisserand et al. 2020; Karambelkar et al. 2021). However, the sample of Galactic dLHdC stars has more than quintupled in the last year with the discovery of 27 new dLHdC stars (Tisserand et al. 2022). Additionally, several new RCB stars have been discovered and observed spectroscopically at near-infrared (NIR) wavelengths (Karambelkar et al. 2021).

⋆ The spectra presented in this paper are also available at the CDS via anonymous ftp to cdsarc.cds.unistra.fr (130.79.128.5) or via https://cdsarc.cds.unistra.fr/viz-bin/cat/J/A+A/667/A84

[1] Historically, dLHdC stars were referred to as HdC stars. Here, we follow the updated nomenclature of Tisserand et al. (2022).

NIR spectroscopic observations were key to identifying He-core and CO-core WD mergers as the progenitors of dLHdC and RCB stars. The *K*-band spectra of these stars show anomalously strong $^{12}C^{18}O$ first overtone bands in addition to the $^{12}C^{16}O$ first overtone bands (Clayton et al. 2005). The values of $^{16}O/^{18}O$ in dLHdC and RCB stars cover a remarkably wide range (from 0.3 to 50), thus in all cases 1–3 orders of magnitude smaller than the solar value (~500). The large amount of ^{18}O is thought to be produced by partial helium burning in a thin shell around the core of the WD merger remnant, which is convectively dredged up to the surface (Clayton et al. 2007; Crawford et al. 2020).

It has been suggested that in addition to dust production, $^{16}O/^{18}O$ ratios could be a second difference between RCB and dLHdC stars. Clayton et al. (2007) and García-Hernández et al. (2009) noted that dLHdC stars have $^{16}O/^{18}O < 1$ and most RCB stars have $^{16}O/^{18}O > 1$. However, this analysis is based on a small sample of only two dLHdC and five RCB stars[2]. Both dLHdC stars in the sample have $^{16}O/^{18}O < 1$, while three of the five RCB stars have $^{16}O/^{18}O > 1$. Karambelkar et al. (2021) measured the ratios for six additional RCB stars using medium resolution spectra and found that they had $^{16}O/^{18}O > 1$. However, additional measurements of these ratios for dLHdC stars were not possible in the past because of the five dLHdC stars known at the time, only three had temperatures cold enough to show the CO bands (Clayton et al. 2007; García-Hernández et al. 2009, 2010).

In this paper, we present the largest sample of $^{16}O/^{18}O$ values in dLHdC and RCB stars measured to date. We use medium resolution NIR spectra to measure $^{16}O/^{18}O$ for seven dLHdC and 33 RCB stars. We also present *JHK*-band spectra of 21 (20 new, one previously known) dLHdC stars for the first time. Our results conclusively show that most dLHdC stars have lower $^{16}O/^{18}O$ than most RCB stars. In Sect. 2, we describe our spectroscopic observations, which include data collected over the last 15 years. In Sect. 3, we describe the NIR spectral features of dLHdC stars. We outline our methods for measuring $^{16}O/^{18}O$ in Sect. 4.1. We discuss the implications of the different oxygen isotope ratios for formation scenarios of RCB and dLHdC stars in Sect. 5, and conclude with a summary of our results in Sect. 6.

2. Data

Our data comprise medium resolution NIR spectra of 24 dLHdC stars and 49 RCB stars. All but two of the stars are resident in the Milky Way; the others are in the Magellanic Clouds. The complete log of spectroscopic observations together with the S/N for each spectrum is presented in Table 1.

The spectra of 18 of the 20 newly discovered dLHdC stars were taken with the Triplespec spectrograph (Herter et al. 2008, $R \approx 3000$) on the 200-inch Hale telescope at Palomar observatory on several nights between June and October 2021. Two newly discovered dLHdC star (A166 and A183) were observed with the SpeX spectrograph ($R \approx 2500$) on the 3 m NASA Infrared Telescope Facility (IRTF, Rayner et al. 2003) on UT 20210623. We include a previously unpublished spectrum of the previously known dLHdC star HD 137613 taken with the UKIRT Imager Spectrometer (UIST, Ramsay Howat et al. 2004, $R \approx 3100$) on the 3.8 m United Kingdom Infrared Telescope (UKIRT) on UT 20050309. We also include spectra of three other previously known dLHdC stars obtained with the Gemini Near-infrared Spectrograph (GNIRS, Elias et al. 2006) on the 8.1 m Gemini-South telescope in the long-slit mode with $R \approx 5900$ in 2005, reported by Clayton et al. (2007).

The spectra of the RCB stars were collected over the last 15 years at three telescopes with four different instruments. We include spectra of six RCB stars obtained with Gemini South/GNIRS in September 2005 (Clayton et al. 2007) and 4 more RCB stars observed with the Flamingos 2 spectrograph (Eikenberry et al. 2004) on the Gemini-South telescope in 2015 and 2016. We observed the RCB star Z Umi with GNIRS on the Gemini-North telescope in 2011. In 2013, we observed nine RCB stars with IRTF/SpeX at $R \approx 2500$. We observed 12 more RCB stars in 2014 and 26 RCB stars in 2015 with IRTF/Spex at $R \approx 5000$.

The Triplespec and IRTF spectra were reduced using the IDL package `spextool` (Cushing et al. 2004), and were flux calibrated and corrected for telluric absorption with standard star observations using `xtellcor` (Vacca et al. 2003). The UKIRT spectrum of HD 137613 was reduced in a standard manner using the Figaro software package for flatfielding, removal of the effects of cosmic ray hits, spectral and spatial rectification of the spectral images, wavelength calibration using an argon lamp, and ratioing by the spectrum of a standard star. The Gemini spectra were reduced similarly, but used a combination of IRAF and Figaro as described in Clayton et al. (2007).

3. NIR spectra of dLHdC stars

We present *JHK*-band NIR spectra of the 20 new dLHdC stars in Fig. 1. We also include in the figure spectra of the previously known dLHdC star HD 137613 (green) and the RCB star NSV11154 (red, taken from Karambelkar et al. 2021).

The spectra of the dLHdC stars closely resemble NIR spectra of RCB stars taken at maximum light. The continuum shapes resemble those of F-G type stars. Numerous absorption lines are present. We identify strong absorption features attributed to C I (most prominently at 1.06883, 1.0686, 1.0688 and 1.06942 μm in the *J*-band and 1.73433, 1.74533 and 1.75104 μm in the *H*-band) and a blend of numerous Fe I, K I and Si I lines (see Rayner et al. 2003 for the wavelengths). H lines are absent in the NIR spectra of the dLHdC stars[3]. Only five of the twenty new dLHdC stars show $^{12}C^{16}O$ and $^{12}C^{18}O$ molecular features (presumably because the others are too hot for CO to exist in detectable amounts). Of the five, all but A166 also show the $^{12}C^{14}N$ bands at 1.0875, 1.0929, 1.0966, 1.0999 μm. Two additional stars B565 and A811 show CN but no CO bands.

Helium 1.0833 μm triplet

Our NIR spectra cover the He I 1.0833 μm triplet. This feature can serve as a tracer of high velocity winds around RCB and dLHdC stars. The levels of this transition are 20 eV above the ground state, and cannot be populated by photospheric radiation of dLHdC and RCB stars. Instead, they can be collisionally excited in high velocity winds around these stars. The He I feature has been observed in several RCB stars either as blueshifted absorption or as a P-Cygni profile with velocities as high as 500 km s^{-1} (Clayton et al. 2003, 2011; Karambelkar et al. 2021). The strength and velocity of the winds around RCB stars are greatest when the stars have just emerged from dust enshrouded minima, and decrease with time thereafter. This suggests that the winds around RCB stars are dust-driven; that is, the gas is

[2] Note that the star HD 175893 was originally classified as a dLHdC star but is now known to be an RCB star based on an IR excess found by Tisserand (2012).

[3] See here for a list of NIR H lines.

Table 1. Log of spectroscopic observations.

Name	Class	Date	S/N	Tel./Inst.	Name	Class	Date	S/N	Tel./Inst.
HD 137613	dLHdC	09/03/2005	>100	UKIRT/UIST	ASAS-RCB-17	RCB	08/2013,06/2015	27	IRTF/SpeX
HD 182040	dLHdC	09/2005	>100	GS/GNIRS	ASAS-RCB-4	RCB	08/2013,06/2015	25	IRTF/SpeX
HD 148839	dLHdC	09/2005	>100	GS/GNIRS	MACHO-401.48170.2237	RCB	08/2013,06/2015	36	IRTF/SpeX
HD 173409	dLHdC	09/2005	>100	GS/GNIRS	ASAS-RCB-14	RCB	08/2013,08/2014	51	IRTF/SpeX
A183	dLHdC	23/06/2021	92	IRTF/SpeX	ASAS-RCB-18	RCB	08/2014	42	IRTF/SpeX
A166	dLHdC	23/06/2021	48	IRTF/SpeX	IRAS18135.5-2419	RCB	08/2014	39	IRTF/SpeX
C17	dLHdC	25/06/2021	44	P200/TSpec	EROS2-CG-RCB-4	RCB	08/2014	48	IRTF/SpeX
A223	dLHdC	25/06/2021	116	P200/TSpec	MACHO-308.38099.66	RCB	08/2014,06/2015	22	IRTF/SpeX
B42	dLHdC	25/06/2021	109	P200/TSpec	WISE_J194218.38−203247.5	RCB	08/2014	68	IRTF/SpeX
A226	dLHdC	25/06/2021	50	P200/TSpec	OGLE-GC-RCB-1	RCB	08/2014,06/2015	62	IRTF/SpeX
C38	dLHdC	29/06/2021	64	P200/TSpec	EROS2-CG-RCB-9	RCB	08/2014	40	IRTF/SpeX
C20	dLHdC	29/06/2021	39	P200/TSpec	EROS2-CG-RCB-11	RCB	08/2014	41	IRTF/SpeX
C105	dLHdC	02/07/2021	140	P200/TSpec	WISE_J183649.54−113420.7	RCB	08/2014	31	IRTF/SpeX
F75	dLHdC	02/07/2021	49	P200/TSpec	V739 Sgr	RCB	08/2014,06/2015	52	IRTF/SpeX
B565	dLHdC	15/09/2021	70	P200/TSpec	V3795 Sgr	RCB	08/2014	67	IRTF/SpeX
B566	dLHdC	15/09/2021	90	P200/TSpec	ASAS-RCB-5	RCB	06/2015	58	IRTF/SpeX
C528	dLHdC	15/09/2021	20	P200/TSpec	ASAS-RCB-7	RCB	06/2015	62	IRTF/SpeX
C539	dLHdC	15/09/2021	46	P200/TSpec	ASAS-RCB-16	RCB	06/2015	59	IRTF/SpeX
A811	dLHdC	15/09/2021	65	P200/TSpec	ASAS-RCB-19	RCB	06/2015	42	IRTF/SpeX
B567	dLHdC	15/09/2021	74	P200/TSpec	ASAS-RCB-20	RCB	06/2015	42	IRTF/SpeX
A798	dLHdC	15/10/2021	47	P200/TSpec	EROS2-CG-RCB-3	RCB	06/2015	73	IRTF/SpeX
C542	dLHdC	15/10/2021	89	P200/TSpec	EROS2-CG-RCB-10	RCB	06/2015	24	IRTF/SpeX
B563	dLHdC	15/10/2021	60	P200/TSpec	EROS2-CG-RCB-13	RCB	06/2015	41	IRTF/SpeX
A814	dLHdC	15/10/2021	50	P200/TSpec	FH Sct	RCB	06/2015	62	IRTF/SpeX
HD 175893	RCB	09/2005	>100	GS/GNIRS	GU Sgr	RCB	06/2015	45	IRTF/SpeX
S Aps	RCB	09/2005	>100	GS/GNIRS	RS Tel	RCB	06/2015	32	IRTF/SpeX
SV Sge	RCB	09/2005	>100	GS/GNIRS	V482 Cyg	RCB	06/2015	25	IRTF/SpeX
ES Aql	RCB	09/2005	>100	GS/GNIRS	V854 Cen	RCB	06/2015	39	IRTF/SpeX
WX CrA	RCB	09/2005	>100	GS/GNIRS	V1783 Sgr	RCB	06/2015	40	IRTF/SpeX
U Aqr	RCB	09/2005	>100	GS/GNIRS	V2552 Sgr	RCB	06/2015	40	IRTF/SpeX
Z Umi	RCB	03/2011	>100	GN/NIRI	VZ Sgr	RCB	06/2015	40	IRTF/SpeX
ASAS-RCB-11	RCB	08/2013	34	IRTF/SpeX	WISE_J174328.50−375029.0	RCB	06/2015	42	IRTF/SpeX
EROS2-CG-RCB-6	RCB	08/2013	26	IRTF/SpeX	V532 Oph	RCB	06/2015	57	IRTF/SpeX
V517 Oph	RCB	08/2013	32	IRTF/SpeX	HV 5637	RCB	11/2015	>50	GS/F-2
V1157 Sgr	RCB	08/2013	39	IRTF/SpeX	EROS2-SMC-RCB-1	RCB	12/2015	>100	GS/F-2
NSV 11154	RCB	08/2013	22	IRTF/SpeX	EROS2-SMC-RCB-2	RCB	10/03/2016	>50	GS/F-2
					EROS2-SMC-RCB-3	RCB	10/09/2016.	>50	GS/F-2

dragged to high velocities by dust grains that are accelerated by radiation pressure. As dLHdC stars do not show dust excesses in their spectral energy distributions, we do not expect to see dust-driven winds around them. Geballe et al. (2009) observed the four previously known dLHdC stars and found no evidence for strong RCB-like He I absorption lines in their spectra.

Figure 2 shows a zoom-in of the NIR spectra of the new dLHdC stars around the He I 1.0833 μm triplet. We do not detect RCB-like (width >200 km s^{-1}) helium absorption in the NIR spectra for any of the newly discovered dLHdC stars, except possibly A166. We cannot determine whether a lower velocity He I component is present in this star from our medium resolution spectra, as we cannot resolve possible contribution of He I to the Si I (1.0831 μm) line. A166 is the only dLHdC star that shows signs of an extended absorption component in addition to Si I absorption. If this is indeed the He I line, it would imply a wind velocity of ≈400 km s^{-1}. Higher resolution observations are necessary to identify the sources of this absorption.

Although we cannot completely resolve any possible low velocity He I component, our observations rule out the presence of strong, RCB-like dust-driven mass loss in dLHdC stars. This is expected, as none of these stars (except A166) shows a significant IR excess (Tisserand et al. 2022). We note, however, that this does not rule out the possibility that dLHdC stars were forming dust at some point in their history (≳10 years ago). Observations of XX Cam – an RCB star that has not entered a dust-enshrouded decline for the last six decades – do not show any significant He I features, similar to dLHdC stars (Geballe et al. 2009). The dust-driven He I wind is thus only a tracer of recent (few years to decades) dust-formation.

4. ^{16}O/^{18}O: Analysis and results

4.1. Analysis

In this section we constrain the ^{16}O/^{18}O ratios of the five newly discovered dLHdC stars that show ^{12}C^{16}O and ^{12}C^{18}O bands, the previously known dLHdC stars HD 137613 and HD 182040 and 33 RCB stars that show the CO bands. Figure 3 shows the first four overtone CO bandheads of the seven dLHdC stars and six representative RCB stars. Even from visual inspection of the spectra, it is evident that in general the ^{12}C^{18}O absorptions are

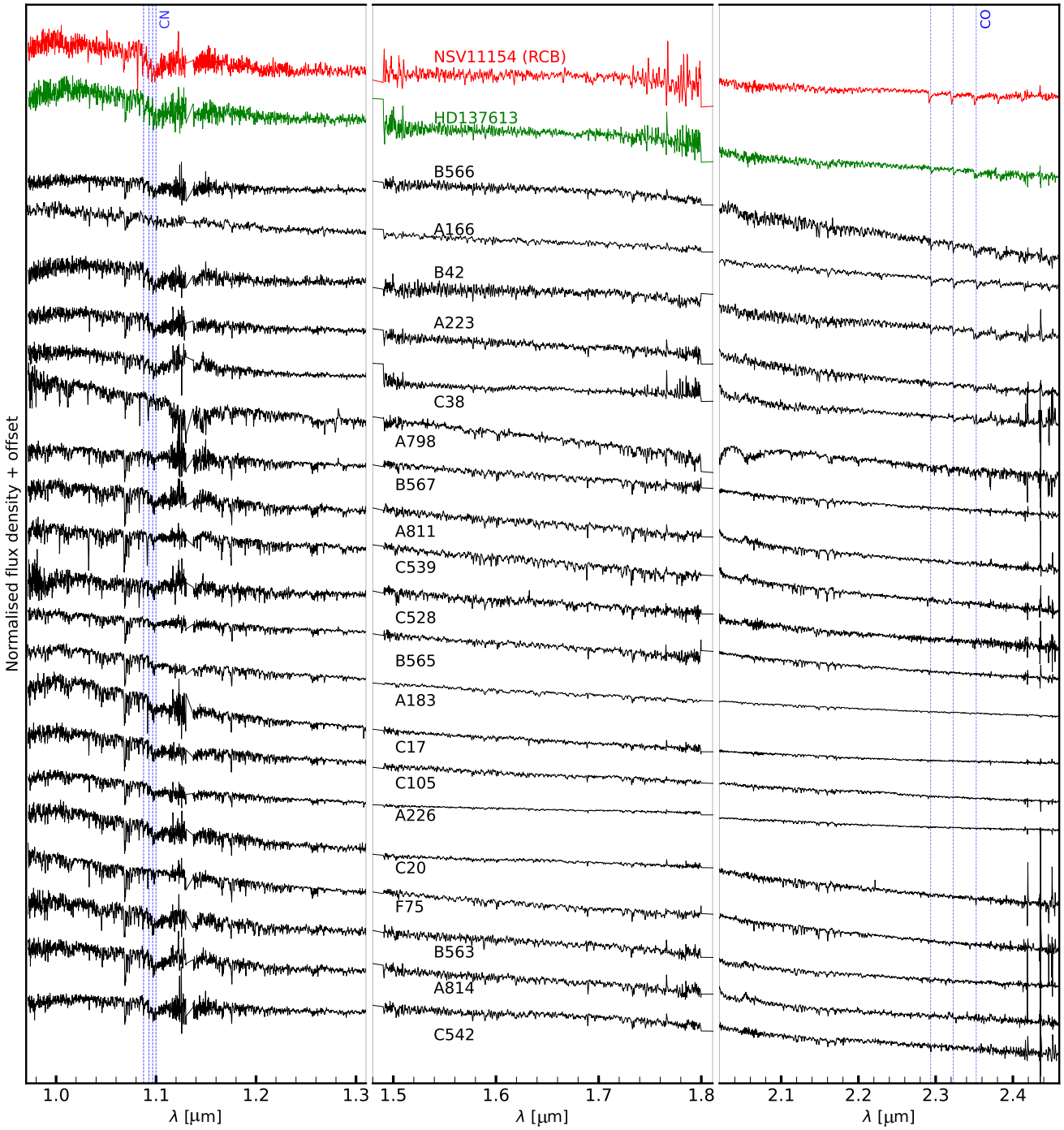

Fig. 1. Near-infrared spectra of the newly discovered dLHdC stars. Near-infrared spectra of the RCB star NSV11154 and the previously known dLHdC star HD137613 are also shown for comparison. The rest-frame positions of the CN and $^{12}C^{16}O$ absorption bands are indicated by dashed vertical lines.

stronger in dLHdC stars than RCB stars. Here, we describe our procedure to derive constraints on the $^{16}O/^{18}O$ ratios from these and other spectra.

We follow the procedure described in Karambelkar et al. (2021). We first generated synthetic spectra using a grid of hydrogen-deficient spherically symmetric MARCS (Model Atmospheres in Radiative and Convective Scheme) atmospheric models with input compositions characteristic of RCB and dLHdC stars ($\log \epsilon(\mathrm{H}) = 7.5$, $\log \epsilon(\mathrm{He}) = 11.5$, log and C/He = 0.01, Gustafsson et al. 1975, 2008; Bell et al. 1976; Plez 2008). The models assumed a solar metallicity to derive compositions of other elements, a total mass of 1 $M_\odot$, $\xi = 5\,\mathrm{km\,s^{-1}}$ and surface gravity $\log g = 1.0$. We generated synthetic spectra using the package `TURBOSPECTRUM` (Alvarez & Plez 1998) and line lists from Goorvitch (1994), Plez (priv. commun. and described in Hedrosa et al. 2013) and Yurchenko et al. (2018) for CO, CN and C_2 molecules respectively. We varied the effective temperatures from 4000 to 7500 K in intervals of 250 K. The C, N and O abundances are relevant to measure the oxygen isotope ratios. However, we cannot measure these abundances from our low to medium resolution spectra directly. We assumed a C/He ratio of 0.01 (Asplund et al. 2000), corresponding to $\log \epsilon(\mathrm{C}) = 9.5$.

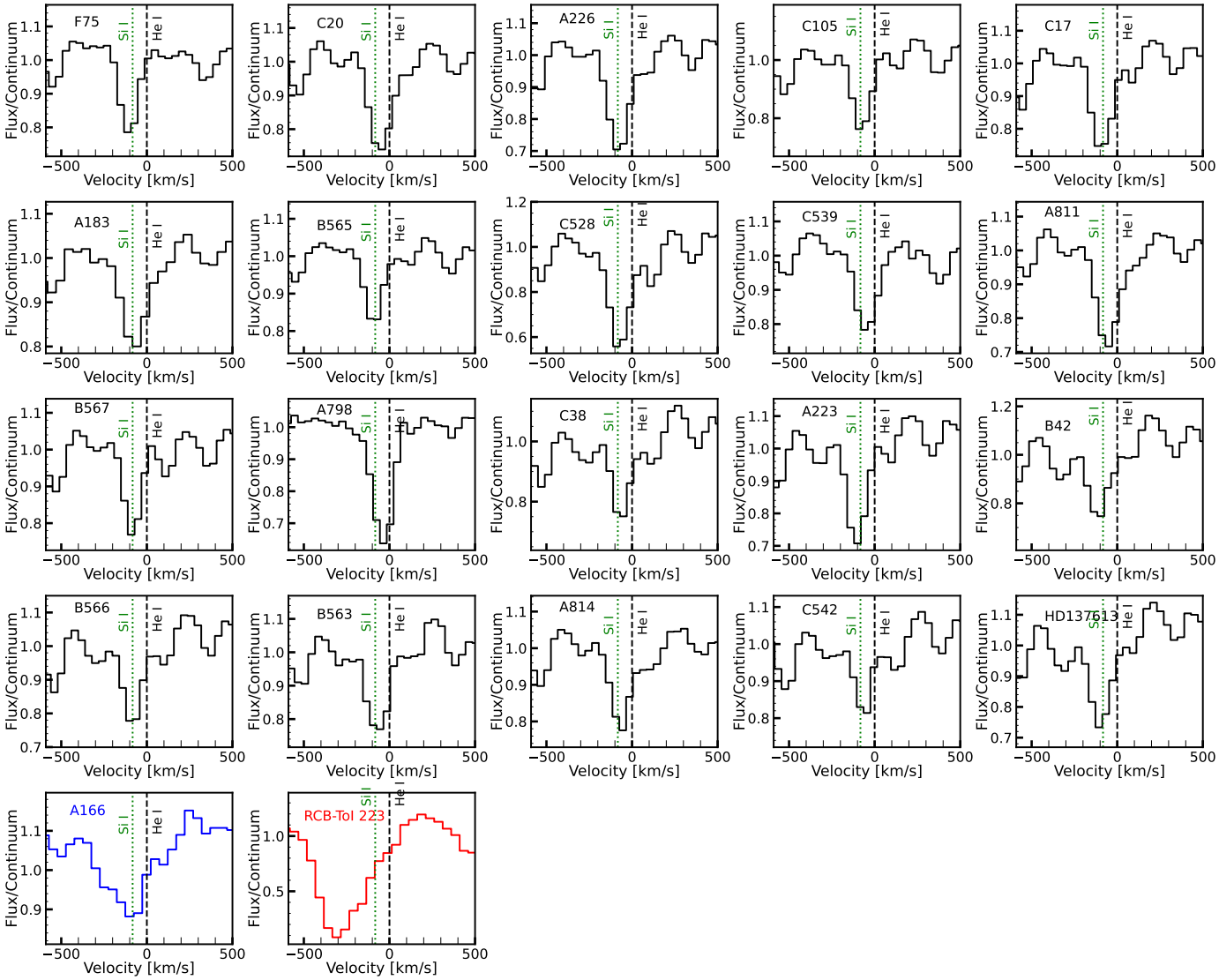

Fig. 2. Zoom-in of the spectral region around the He I (10 833 Å) triplet. The velocity is measured with respect to 1.0833 µm. The same spectral region of He I profile of an RCB star is shown in red – RCB-ToI-223 (a.k.a. WISE J182010.96−193453.4), at a phase when it has just emerged from a dust decline. We cannot resolve the contribution from the Si I line to any He I features from our low resolution spectra. However, it is evident that we do not detect any strong (>200 km s^{-1}), RCB-like winds in any dLHdC star, suggesting that there are no dust-driven winds around them. This is consistent with no hot dust excesses seen in the SEDs of any of these stars. A166 is the only dLHdC star that shows a possible high velocity He I absorption profile (plotted in blue).

We also fixed the total oxygen abundance to log ϵ(O) = 8.8 (consistent with the range of observed O abundances for RCB stars Asplund et al. 2000), and only varied the oxygen isotope ratios to vary the relative contribution of ^{16}O and ^{18}O. We chose ^{16}O/^{18}O values of 0.01, 0.05, 0.1, 0.2, 0.5, 1, 2, 5, 10, 20, 50, 500 and infinity (no ^{18}O). Finally, to partially mitigate the effects of fixing the abundances, we varied the nitrogen abundances, choosing values of log ϵ(N) = 7.0, 7.5, 8.0, 8.5 and 9.4 (Asplund et al. 2000) Additionally, for RCB stars, the warm dust shell can contribute significantly to the K-band flux (up to 80%, Tisserand et al. 2013), veiling the absorption bands. To account for this, we introduced an additional parameter $f_{\rm dust} = \frac{F_{\rm shell,K}}{F_{\rm total,K}}$, and varied it between 0 and 0.8 in steps of 0.1 for RCB stars. We do not expect this to be a significant effect for dLHdC stars as they do not have infrared dust excesses. We fit the synthetic spectra to continuum-normalised NIR spectra and visually examine each of the fits to determine the range of isotope ratios that is consistent with the observed spectra. We are only able to place wide range estimates on the oxygen isotope ratios owing to the several free parameters and assumptions in our fitting. Future higher resolution spectra will determine the CNO abundances precisely and provide precise oxygen isotope ratios for the stars presented here. The derived values of ^{16}O/^{18}O are listed in Table 2, and Figs. 4, 5 and 6 show some examples of the model fits.

As noted in García-Hernández et al. (2009), it is challenging to measure the ^{16}O/^{18}O ratios accurately from medium resolution spectra. The ^{12}C^{16}O and ^{12}C^{18}O absorption bands can be contaminated by absorption from other molecules such as ^{12}C^{14}N and C_2. The absorption lines of CN and C_2 are densely packed in the K band. It is also possible that the ^{12}C^{16}O absorption bands are saturated, resulting in a smaller measured ^{16}O/^{18}O ratio than the true value. There is also a degeneracy between the effects of the effective temperatures and nitrogen abundances on the depths of the CO absorption bands. For these reasons, we are not able to tightly constrain ^{16}O/^{18}O, but instead provide a range of values combining the effects of the temperatures, nitrogen

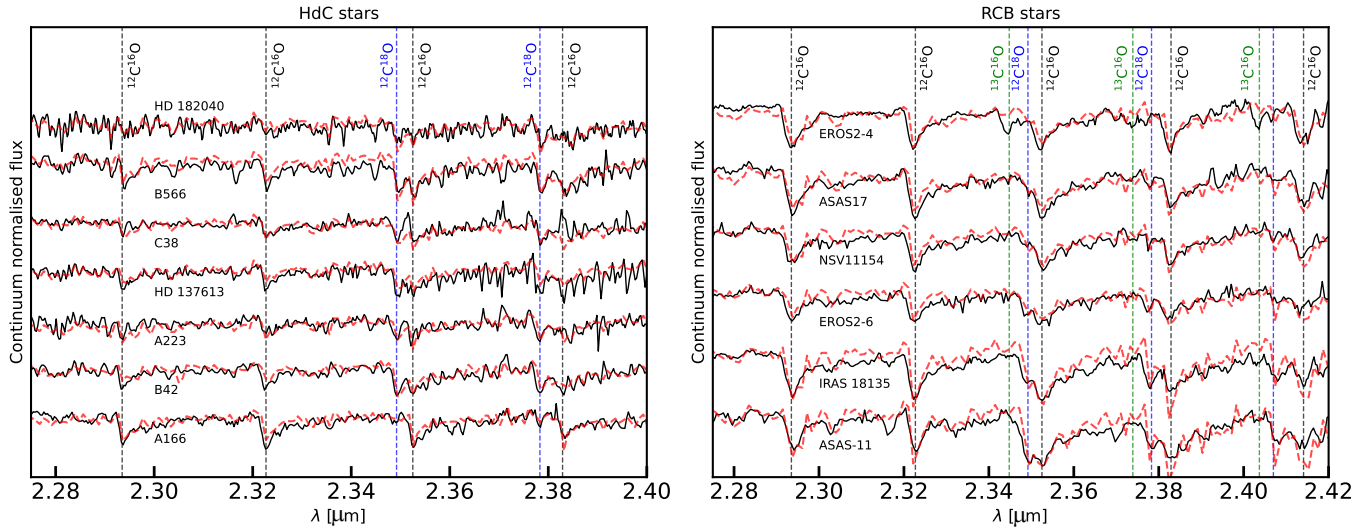

Fig. 3. Zoom-in of the $^{12}C^{16}O$ and $^{12}C^{18}O$ absorption bands of all seven dLHdC stars (*left*) and six representative RCB stars (*right*) from our sample. All dLHdC stars except A166 show strong $^{12}C^{18}O$ absorption, comparable in strength to the $^{12}C^{16}O$ absorption. The RCB stars show a range of $^{12}C^{18}O$ absorption strengths. Shown are two RCB stars where the $^{12}C^{18}O$ absorption is strongest, two where it is of intermediate strength and two where the absorption is weak. Of the 33 RCB stars analyzed here, only five have strong dLHdC-like $^{12}C^{18}O$ absorption, while the remaining majority has intermediate or weak $^{12}C^{18}O$ absorption. We also plot examples of synthetic spectra that fit the observed spectra as red dashed lines. Note that the RCB star EROS2-CG-RCB4 shows $^{13}C^{16}O$ absorption bands (*right panel*).

abundances and $f_{\rm dust}$. Wherever possible, we use estimates of temperature ranges from the literature to tighten the constraints. Despite the wide range of ratios for each star, our measurements strongly suggest that most dLHdC stars have significantly lower $^{16}O/^{18}O$ than RCB stars.

4.2. Results

4.2.1. dLHdC stars

With the exception of A166, the depths of the $^{12}C^{18}O$ absorption bands in the dLHdC stars are comparable to those of the $^{12}C^{16}O$ bands (see Fig. 3). We use temperature estimates from the $V-I$ color calibration of the HdC spectral classification system found in Crawford et al. (in prep.). From comparisons to synthetic spectra we derive $^{16}O/^{18}O$ ratios in the ranges 0.05–0.2 for B42, C38 and B566, 0.1–0.5 for A223, HD 182040 and HD 137613. Our derived values for HD 137613 and HD 182040 are consistent with those reported by Clayton et al. (2007) from medium resolution and García-Hernández et al. (2009) from high resolution spectra.

For B42, none of the spectral models fit the CO features at 2.349 μm and 2.352 μ. This could be because the 2.352 μm $^{12}C^{16}O$ band is saturated. Fits to the 2.378 and 2.383 μm bands suggest $^{16}O/^{18}O = 0.05$–0.2, but the only models that fit these bands have a low nitrogen abundance of $\log \epsilon(N) = 7.0$. The optical spectrum of B42 shows strong CN bands (see Tisserand et al. 2022), suggesting that the nitrogen abundance may not be so low. It is possible that the 2.383 μm $^{12}C^{16}O$ band in B42 is also saturated, and the value we report is lower than the true $^{16}O/^{18}O$. If this is the case, our reported uncertainty on the $^{16}O/^{18}O$ of B42 is also likely underestimated, as it does not include the systematic uncertainty associated with the saturated bands and the nitrogen abundances. Higher resolution observations are necessary to measure the true nitrogen abundance and the true $^{16}O/^{18}O$ value of B42.

Unlike the other dLHdC stars, A166 shows significantly weaker $^{12}C^{18}O$ absorptions than the $^{12}C^{16}O$ absorption; we constrain $^{16}O/^{18}O > 20$ for this star. Tisserand et al. (2022) note that A166 is an outlier among the newly discovered dLHdC stars. In the HR diagram, it is located near two cool RCB stars and is distant from most dLHdC stars. It also has IR excesses in the WISE W3 and W4 bands. This, together with its high, RCB-like value of $^{16}O/^{18}O$ and possible broad He I absorption suggests that it is an RCB star. However, the lack of IR excesses in the NIR and WISE W1 and W2 bands indicates that it is in a phase of low dust production, similar to XX Cam (see Sect. 4.6 of Tisserand et al. 2022).

4.2.2. RCB stars

Of the 33 RCB stars that show the CO overtone absorption bands, estimates of effective temperatures are available for 19 (Crawford et al., in prep.). We are able to derive the tightest constraints on $^{16}O/^{18}O$ for them. For most of the remaining 12, we can only derive lower limits on $^{16}O/^{18}O$.

Most of the RCB stars in our sample have much weaker $^{12}C^{18}O$ absorption bands relative to $^{12}C^{16}O$, than dLHdC stars. A total of 28 of the 33 RCB stars have $^{16}O/^{18}O > 1$. Eight of them do not show any $^{12}C^{18}O$ bandheads in our medium resolution spectra, and are consistent with the $^{16}O/^{18}O \gtrapprox 500$ models. Figure 6 shows a zoom-in of the spectrum of one such star. However, it is possible that these measurements are not accurate for the following reasons. First, it is possible that the resolution and S/N of these spectra is not sufficient to resolve a weak $^{12}C^{18}O$ bandhead from the $^{12}C^{14}N$ bands (that are possibly enhanced by the low effective temperatures) in this region of these cold stars. Second, it is possible that the strong CO bandheads in the spectra of these cold RCB stars are saturated. As our medium resolution spectra cannot resolve the weaker, unsaturated CO lines, we cannot accurately measure their oxygen isotope ratios. Third, it is also possible that the spectra of these cold stars suffer strong dust dilution, making it difficult to detect the diluted $^{12}C^{18}O$ bandheads at medium resolution. We caution that a combination of these resolution, saturation and dilution effects could be preventing the detection of $^{12}C^{18}O$ bands in our spectra of these cold stars. Higher resolution spectra are required to obtain

Table 2. Range of model parameters that best fit the observed spectra.

Name	Class	Temperature	log(ϵ(N))	f_{dust}	$^{16}O/^{18}O$
B42 [a]	dLHdC	4500–5000 [c]	7.0–7.5	0	0.01–0.1
C38	dLHdC	5000–5800 [c]	9.4	0	0.05–0.2
B566	dLHdC	5000–5800 [c]	9.4	0	0.05–0.5
HD 137613	dLHdC	4500–5000 [c]	7.5–9.4	0	0.05–0.5
A223	dLHdC	5000–5800 [c]	9.4	0	0.2–1
HD 182040	dLHdC	5000–5800 [c]	8.5–9.4	0	0.1–0.5
A166	dLHdC	4000–6000 [d]	7.0–9.4	0	>20
HD 175893	RCB	4500–5000 [c]	7.0–9.4	0–0.5	0.01−0.2
ASAS-RCB-11	RCB	4500–5000 [c]	7.0–9.4	0–0.3	0.01−0.2
WX Cra	RCB	4100-4500 [c]	7.0–9.4	0–0.2	0.05−1
EROS2-CG-RCB-6	RCB	4500–5750 [d]	7.0–9.4	0–0.8	0.2−5
IRAS 1813.5-2419	RCB	3900–4100 [c]	7.0–9.4	0–0.5	0.2−20
S Aps [a]	RCB	4100–4500 [c]	7.0	0–0.8	1−5
SV Sge [a]	RCB	3900–4100 [c]	7.0–9.4	0	1−5
HV 5637	RCB	4500–5750 [d]	7.0–9.4	0–0.8	1−50
ES Aql [a]	RCB	4500–6000 [d]	7.0–9.4	0–0.3	2−20
Z Umi	RCB	4750–5500 [d]	9.4	0.5-0.8	1−20
EROS2-SMC-RCB-2	RCB	4500–6000 [d]	7.0–9.4	0–0.8	2−50
EROS2-SMC-RCB-3	RCB	5250–6000 [d]	9.4	0.5-0.8	5−50
V1783 Sgr	RCB	4100–4500 [c]	9.4	0.7-0.8	5−50
U Aqr	RCB	4100–4500 [c]	9.4	0.4-0.8	5−50
EROS2-CG-RCB-10	RCB	4500–5750 [d]	7.0–9.4	0–0.8	5−50
ASAS-RCB-17	RCB	4100–4500 [c]	7.0–9.4	0–0.1	5−50
NSV 11154	RCB	5250–5500 [e]	7.0–9.4	0–0.2	10−50
V1157 Sgr	RCB	3900–4100 [c]	7.0–9.4	0–0.8	>10
ASAS-RCB-16	RCB	4100–4500 [c]	7.0	0	>20
MACHO-401.48170.2237	RCB	4500–6000 [d]	7.0–9.4	0–0.8	>20
ASAS-RCB-18	RCB	3750–3900 [c]	7.0–9.4	0–0.8	>20
WISE_J174328.50-375029.0	RCB	3900–4100 [c]	7.0–9.4	0–0.6	>50
ASAS-RCB-19	RCB	3750–3900 [c]	7.0–9.4	0.5-0.6	>50
MACHO-308.38099.66	RCB	4000–5500 [d]	7.0–9.4	0–0.8	>50
ASAS-RCB-4	RCB	3750–3900 [c]	7.0–9.4	0–0.2	>50
EROS2-CG-RCB-13 [f]	RCB	4500–5500 [d]	7.0–9.4	0–0.8	>500
EROS2-CG-RCB-3 [f]	RCB	6000–6500 [d]	9.4	0–0.3	>500
EROS2-CG-RCB-4 [b] [f]	RCB	4500–5500 [d]	7.0–9.4	0–0.8	>500
V517 Oph [f]	RCB	4500–5500 [d]	7.0–9.4	0–0.8	>500
ASAS-RCB-7 [f]	RCB	3750–3900 [c]	7.0–9.4	0–0.8	>500
OGLE-GC-RCB-1 [f]	RCB	4100–4500 [c]	7.0–9.4	0–0.4	>500
ASAS-RCB-5 [f]	RCB	3900–4100 [c]	7.0–9.4	0–0.6	>500
WISE_J194218.38-203247.5 [f]	RCB	3900–4100 [c]	7.0–9.4	0–0.8	>500

Notes. [a]The $^{12}C^{16}O$ absorption bands are possibly saturated, and the $^{16}O/^{18}O$ is likely underestimated. [b]EROS2-CG-RCB-4 shows $^{13}C^{16}O$ absorption bands. [c]Photometry based temperature range estimates from Crawford et al. (in prep). [d]Temperature ranges based on the models that are good fits to the NIR spectra. [e]Temperature range from SED fit in (Karambelkar et al. 2021). [f]The medium resolution spectra do not show any strong $^{12}C^{18}O$ bandheads, but it is possible that these bands are not detected due to a combination of low resolution, low S/N, saturation and dust-dilution of CO bandheads (see Sect. 4.2.2).

reliable measurements of oxygen isotope ratios in these stars, which we highlight in Table 2. However, it is unlikely that they have very strong dLHdC-like $^{12}C^{18}O$ bands. Thus, the medium resolution spectra suggest that a large majority of RCB stars have higher $^{16}O/^{18}O$ than dLHdC stars.

Five RCB stars – HD 175893, ASAS-RCB-11, IRAS 18135.5-2419, WX CrA and EROS2-CG-RCB-6 – have prominent $^{12}C^{18}O$ absorption features and are consistent with $^{16}O/^{18}O < 1$. We derive $^{16}O/^{18}O$ values of 0.01–0.2, 0.01–0.2, 0.5–5, 0.05–1 and 0.2–5 for these stars, respectively. These values are similar to those of dLHdC stars. We note that our derived $^{16}O/^{18}O$ values for HD 175893, S Aps, SV Sge, ES Aql, U Aqr, Z Umi and WX Cra agree with previous medium resolution measurements from Clayton et al. (2007). Our derived values also agree with high resolution measurements for all of these except S Aps, SV Sge and ES Aql, as the $^{12}C^{16}O$ bandheads are saturated in these three (García-Hernández et al. 2010). Finally, the RCB star EROS2-CG-RCB-4 shows the $^{13}C^{16}O$ absorption bandhead at 2.345, 2.374, 2.404 and 2.434 μm (see Fig. 3).

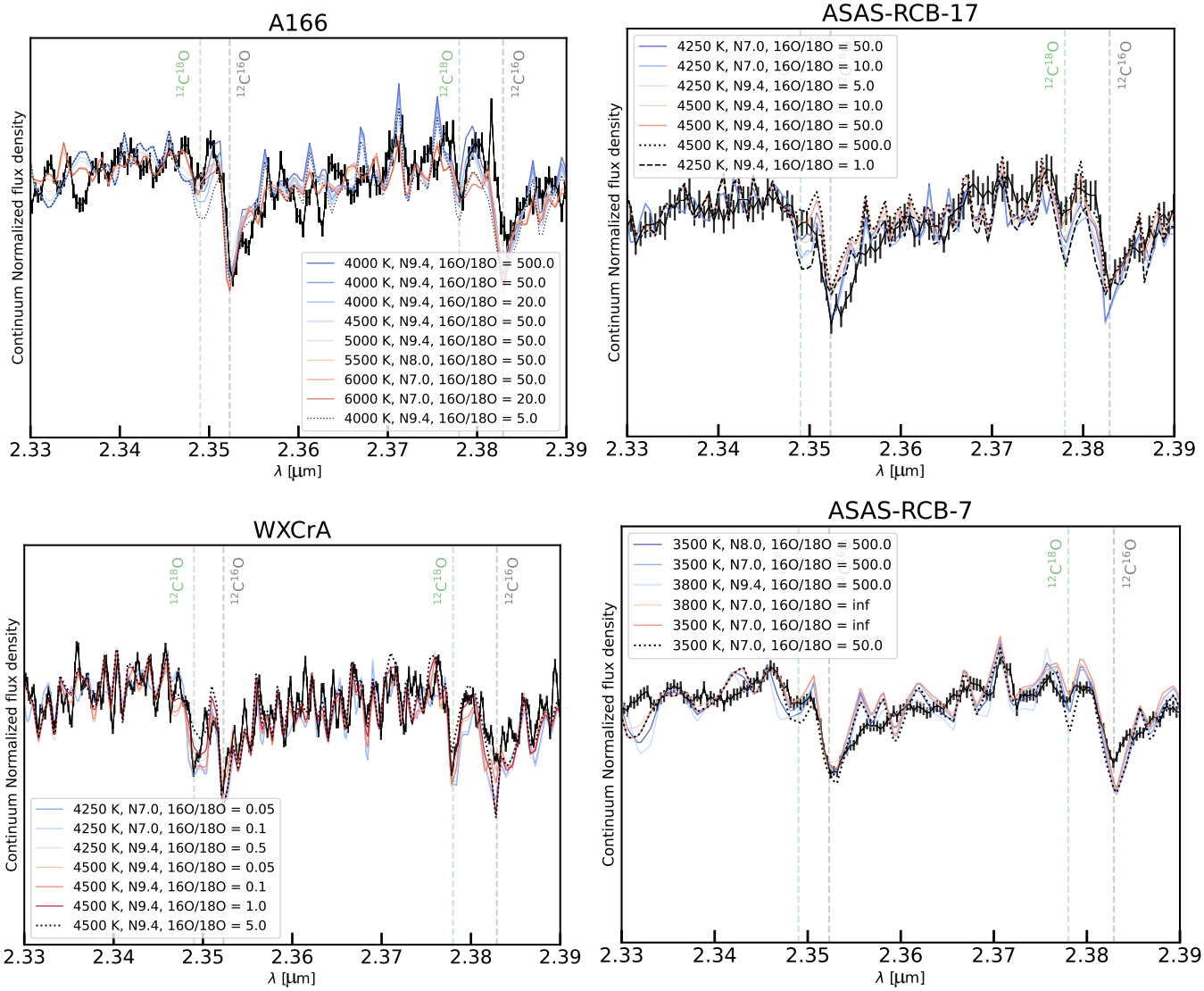

Fig. 4. Model fits to the CO absorption bandheads of the dLHdC star A166 and RCB stars ASAS-RCB-17, WXCrA and ASAS-RCB-7. The spectra (with errorbars) are plotted in black, and the best-fit models for a wide allowed range of model parameters (Table 2) are plotted as solid colored lines. The measured $^{16}O/^{18}O$ for these stars are > 20, $5-50$, $0.05-1$ and > 500 respectively. The dotted and dashed lines show models with oxygen isotope ratios outside these derived ranges ($^{16}O/^{18}O = 10$ for A166, 1 and 500 for ASAS-RCB-17, and 5 for WXCrA). It is challenging to distinguish between models with different N abundances given the medium resolution and S/N of the spectra. We focus on the regions around the $^{12}C^{18}O$ and $^{12}C^{16}O$ bandheads (dashed green and gray lines) and report the range of values consistent with the observed spectra.

To summarize, we find that most dLHdC stars have $^{16}O/^{18}O < 1$, lower than most RCB stars. However, there is an overlap – a small fraction of dLHdC stars have $^{16}O/^{18}O > 1$ while a small fraction of RCB stars have $^{16}O/^{18}O < 1$. We illustrate this in Fig. 7. Finally, we emphasize that high resolution spectra are required to confirm the oxygen isotope ratio measurements, especially in the case of stars that have low effective temperatures. High-resolution spectra will help identify the stars for which the bandheads are saturated, and also provide accurate O and N abundance measurements which are crucial for precise $^{16}O/^{18}O$ measurements. These observations should help confirm our conclusion that most dLHdC stars have smaller $^{16}O/^{18}O$ than most RCB stars.

5. Discussion

Our NIR spectroscopic observations have revealed that in addition to dust-formation, dLHdC and RCB stars can in most cases be distinguished based on their values of $^{16}O/^{18}O$. dLHdC stars in general have a lower $^{16}O/^{18}O$ than RCB stars. It is not surprising that the oxygen isotope ratios are an important factor in the study of dLHdC and RCB stars. Anomalously low $^{16}O/^{18}O$ in dLHdC and RCB stars was key to identifying the merger of a He-core and a CO-core white dwarf as their formation channel.

^{18}O is synthesized by the partial helium burning reaction $^{14}N(\alpha,\gamma)\,F^{18}(\beta^+\nu)^{18}O$. This reaction is efficient at temperatures of $\approx 10^8$ K (Clayton et al. 2007; Jeffery et al. 2011). At higher temperatures, ^{18}O is burnt to ^{22}Ne. These conditions can be achieved in a thin helium burning shell around the merger remnant of a He-core and a CO-core white dwarf (Clayton et al. 2007). The ^{18}O is convectively dredged up to the surface of the star within the first few hundred years after the white dwarf merger (Crawford et al. 2020; Munson et al. 2021; Lauer et al. 2019). The photospheric value of $^{16}O/^{18}O$ in dLHdC and RCB stars is thus set within the first hundred years and remains constant for the rest of their lifetimes ($\approx 10^{4-5}$ years). Here, we

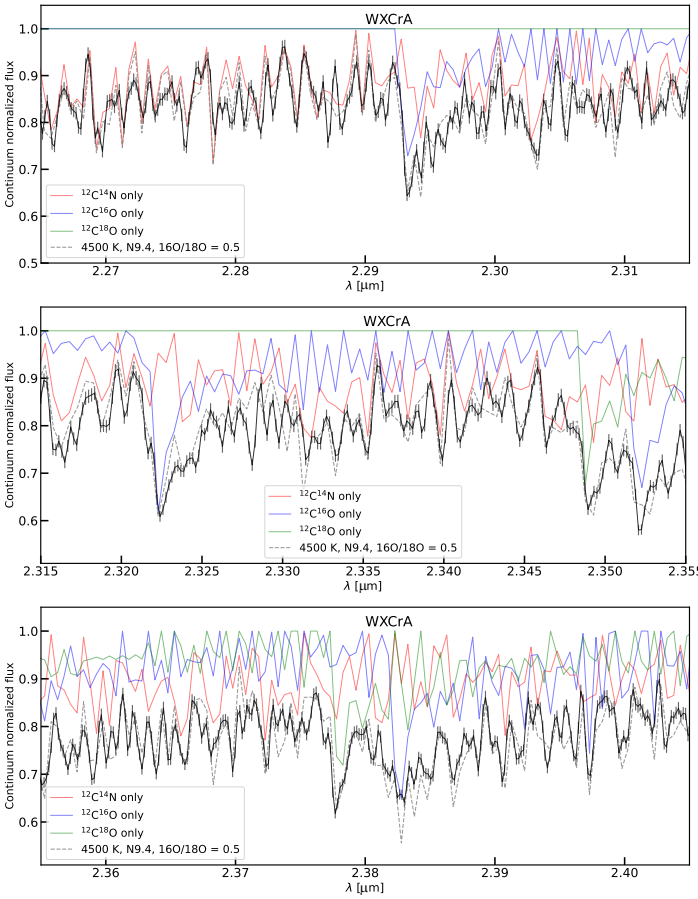

Fig. 5. Zoom-in of the spectra of the RCB star WXCrA (solid black line). We plot the best fit-model synthetic spectrum to this star (gray, dashed line), and show the contribution of $^{12}C^{14}N$ (solid red), $^{12}C^{16}O$ blue and $^{12}C^{18}O$ green. The top, middle and bottom panels show different spectral regions.

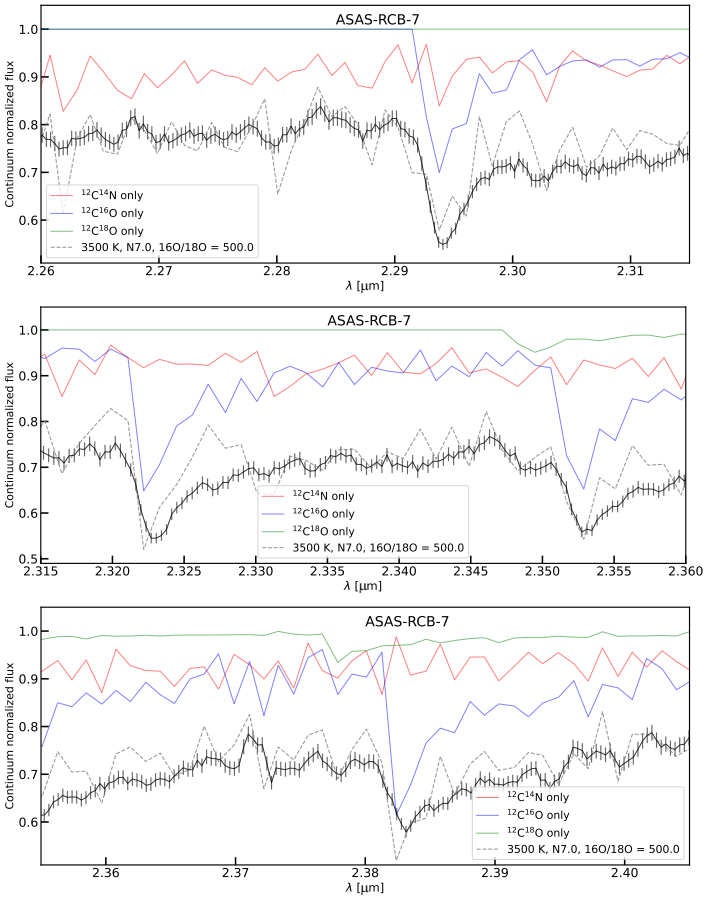

Fig. 6. Zoom-in of the spectra of the RCB star ASAS-RCB-7 (solid black line). We plot the best fit-model synthetic spectrum to this star (gray, dashed line), and show the contribution of $^{12}C^{14}N$ (solid red), $^{12}C^{16}O$ blue and $^{12}C^{18}O$ green. Unlike WXCrA (Fig. 5), this spectrum does not show very strong $^{12}C^{18}O$ bandheads. As our oxygen ratio measurements are based on these bandheads, we estimate $^{16}O/^{18}O \geq 500$ for this source. It is possible that the low spectroscopic resolution and S/N of this spectrum cannot resolve the blended weak bandhead. Higher resolution spectra are required to measure the ratio accurately. The other targets with $^{16}O/^{18}O \geq 500$ could also be affected by a similar issue.

explore the properties of the merging white dwarfs that set the values of $^{16}O/^{18}O$ in the remnant supergiants. We also discuss the implications of our observations on the dLHdC–RCB connection.

5.1. The origin of different $^{16}O/^{18}O$ for dLHdC and RCB stars

Studies have just begun to examine the quantities that affect $^{16}O/^{18}O$ in white dwarf merger remnants. The effects on $^{16}O/^{18}O$ of the helium burning shell temperature, convective extent of the supergiant envelope and the amount of hydrogen in the shell have been explored (Crawford et al. 2020; Munson et al. 2021). Their values in turn depend on the properties of the merging He-core and CO-core white dwarfs, such as their masses, mass ratios and compositions. The different values of $^{16}O/^{18}O$ in dLHdC and RCB stars thus suggest a correlation between the progenitor white dwarfs' properties and dLHdC/RCB formation, which we discuss here. Note however that there are several additional factors that could contribute to the oxygen isotope ratios and remain to be modeled. A large unmodeled source of uncertainty is the effect of the initial composition of the progenitor white dwarfs and post-merger remnant on $^{16}O/^{18}O$. The correlations that we discuss below are based on current understanding and are hence preliminary. Nevertheless, they demonstrate that different properties of merging white dwarfs can result in different values of $^{16}O/^{18}O$, possibly providing a natural explanation for dLHdC vs. RCB formation. Additional modeling will help establish robust relations between progenitor properties and dLHdC–RCB stars.

Crawford et al. (2020) explored the effect of the temperature of the helium burning shell (T_{He}) on $^{16}O/^{18}O$. In particular, $^{16}O/^{18}O$ drops below unity for shell temperatures in the range $T_{He} \approx 2.5–3.5 \times 10^8$ K. Thus, dLHdC stars could be associated with WD merger remnants that have T_{He} in this range. For shell temperatures outside this range, $^{16}O/^{18}O$ increases to RCB-like values, suggesting that RCB stars either have $T_{He} < 2.5 \times 10^8$ K or $T_{He} > 3.5 \times 10^8$ K.

From simulations of white dwarf mergers, Staff et al. (2012) found that T_{He} is inversely correlated with the mass ratio ($q = M_{He}/M_{CO}$, where M_{He} and M_{CO} are the masses of the He white dwarf and CO white dwarf, respectively). They derive values of $T_{He} = 3$, 2.5 and 1.5×10^8 K for $q = 0.5$, 0.6 and 0.7 respectively. The helium shell temperatures of dLHdC stars are consistent with mass ratios $0.5 < q < 0.6$. RCB stars are consistent either with $q > 0.6$ or $q < 0.5$ depending on whether they have $T_{He} < 2.5 \times 10^8$ K or $T_{He} > 3.5 \times 10^8$ K, respectively. However the Staff et al. (2012) analysis does not include an important factor – additional energy contributions from nucleosynthesis in the

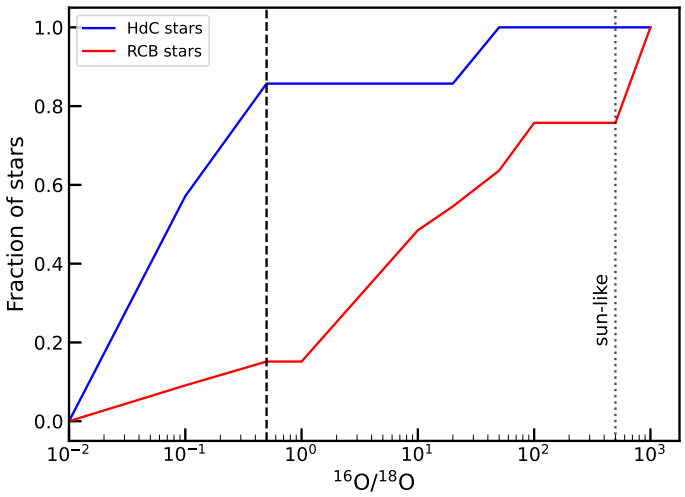

Fig. 7. Cumulative distribution plot showing the fraction of dLHdC and RCB stars that have $^{16}O/^{18}O$ below a given value. Of the dLHdC stars, 85% (6 out of 7) have $^{16}O/^{18}O < 0.5$ (black dashed line) while only $\approx$ 15% of RCB stars (5 out of 33) are consistent with such low $^{16}O/^{18}O$ values. Most dLHdC stars have a lower $^{16}O/^{18}O$ than most RCB stars. A166 is the only dLHdC star that has $^{16}O/^{18}O > 1$. This star is an outlier amongst the newly discovered dLHdC stars, and is likely an RCB star in a low phase of dust production (see Sec. 4.1).

shell. This additional energy will increase the shell temperature, and thus the above estimates of T_{He} are likely lower limits, and the q ranges are unrealistic. No studies of temperature increase due to nucleosynthesis exist in literature.

To first order, we can estimate the temperature increase timescale assuming triple-α burning is the dominant nucleosynthetic energy source (Hansen et al. 2004). Assuming the shell parameters from Staff et al. (2012) and a 100% energy to temperature conversion, we find that the temperature of a $q = 0.7$ merger with initial $T_{He,init} = 1.5 \times 10^8$ K doubles within the first few years after merger. This time reduces to a few days for $q = 0.6$ ($T_{He,init} = 2 \times 10^8$ K) and a few minutes for $q = 0.5$ ($T_{He,init} = 3 \times 10^8$ K). The shell-burning temperatures for $q < 0.6$ mergers can thus exceed 4×10^8 K. RCB stars would then be consistent with low mass-ratio ($q < 0.6$) mergers and dLHdC stars would be consistent with higher mass-ratio mergers ($q > 0.7$)[4]. More detailed studies of nucleosynthetic energy production are required to determine the exact ranges of q that might form RCB and dLHdC stars

T_{He} also depends on the total mass of the white dwarf merger (Staff et al. 2018); however, the exact dependence has not been studied extensively. The Staff et al. (2012) estimates mentioned above assumed $M_{tot} \approx 0.9\,M_\odot$. Without including nucleosynthetic energy, Staff et al. (2018) found that a $M_{tot} = 0.7\,M_\odot$, $q = 0.5$ merger has $T_{He} < 2 \times 10^8$ K – lower than the estimate of 3×10^8 K for the $0.9\,M_\odot$, $q = 0.5$ merger. This suggests that lower mass mergers have lower T_{He} than higher mass mergers. Adding nucleosynthetic energy can increase T_{He} for the $0.7\,M_\odot$ merger to the dLHdC range ($2.5–3.5 \times 10^8$ K) and the $0.9\,M_\odot$ merger outside this range. dLHdC stars would then be consistent with arising from lower mass mergers than RCB stars. This would be consistent with the observation in Tisserand et al. (2022) that the population of dLHdC stars has lower luminosities than RCB stars, which they interpret as a consequence of dLHdC stars originating from lower mass mergers than RCB stars.

In addition to T_{He}, $^{16}O/^{18}O$ can also depend on the extent of the convective envelope and the mass of hydrogen in the helium burning shell (Zhang et al. 2014; Munson et al. 2021). Munson et al. explored the effect of convective overshoot factor (f) on $^{16}O/^{18}O$. They found that for $f < 0.07$, $^{16}O/^{18}O \approx 1$, but increases rapidly for $f > 0.07$. Large values of f correspond to cases where the convective envelope extends all the way to the CO core and dredges up additional ^{16}O from the core into the envelope. The high values of $^{16}O/^{18}O$ in RCB stars could be partly explained due to such a deep convective dredge up. That will also reduce C/O in RCB stars compared to dLHdC stars. The initial conditions of a merging system that would give rise to a deep convective zone remain to be explored. Munson et al. (2021) also showed that $^{16}O/^{18}O$ increases with increasing mass of hydrogen in the helium-burning shell. The presence of hydrogen leads to a decrease of ^{18}O and increase in ^{16}O due to proton capture reactions. The source of this hydrogen is a thin hydrogen envelope around the progenitor He white dwarf (Zhang et al. 2014). The mass of the hydrogen envelope is inversely correlated with the mass of the He white dwarf (Staff et al. 2012; Driebe et al. 1998). However, a significant fraction of this hydrogen is expected to be burned during the merger. How much of the envelope hydrogen actually reaches the helium shell is not known.

In conclusion, the $^{16}O/^{18}O$ values in white dwarf merger remnants are affected by the properties of the merging white dwarfs such as their total mass, mass ratios and individual compositions. In this context, the different values of $^{16}O/^{18}O$ in dLHdC and RCB stars indicate that they are formed from distinct populations of progenitor white dwarf binary mergers.

5.2. The evolutionary link between dLHdC and RCB stars

García-Hernández et al. (2010) speculated the possibility of an evolutionary link between dLHdC and RCB stars. This was based on their surface abundances, together with the assumptions that dLHdC → RCB (→ Extreme Helium Stars) is the common sequence and that their surface abundances change with evolution. They note that depending on the masses and compositions of the merging white dwarfs, the merger remnant will have different initial temperatures on the supergiant track. They associate dLHdC stars with the cooler parts of the supergiant track and RCB stars with hotter temperatures. In their model, depending on merger conditions the merger may first form a cold dLHdC star and eventually evolve to an RCB star, or directly form an RCB star.

The new observations, if corroborated by high-resolution spectroscopy, would show that the picture of a dLHdC-RCB evolutionary link could be incorrect. First, several newly discovered dLHdC stars have higher photospheric temperatures than many RCB stars (Tisserand et al. 2022). Second, the spectra presented and analyzed here demonstrate that dLHdC stars in general may have different values of $^{16}O/^{18}O$ than RCB stars (Sect. 4.1). In addition, recent theoretical modeling by Crawford et al. (2020) suggest that the surface abundances of dLHdC and RCB stars remain constant throughout their lifetimes; that is, it would not be possible for one class to evolve into another.

Instead, we propose that whether a white dwarf merger forms a dLHdC or an RCB depends solely on the properties of the merging white dwarfs. The merger forms a dLHdC star (no significant dust formation, low $^{16}O/^{18}O$) or an RCB star (dust

[4] Note that for mergers where $T_{He} > 4.5 \times 10^8$ K, other elemental abundances predicted by models do not agree with the observed RCB abundances (Crawford et al. 2020). This suggests that there is a lower limit on the mass-ratios of white dwarf binaries that can produce RCB/dLHdC stars.

formation, high $^{16}O/^{18}O$) based on the mass ratios, masses and compositions of the white dwarfs. In this picture, it is still a mystery why RCB stars form large amounts of dust while dLHdC stars do not. It seems reasonable to expect that only those white dwarf mergers that are more massive than a certain threshold or have particular ranges of chemical compositions form remnants that can undergo dust formation. Future theoretical models and studies that more precisely identify the differences between dLHdC and RCB star progenitors could provide an answer to this question.

5.3. The overlap between dLHdC and RCB stars

An intriguing observation is the five RCB stars (classified based on their observed IR excesses and brightness declines) that show low, dLHdC-like $^{16}O/^{18}O$. These "overlap" stars may be a consequence of there being several different factors that contribute to $^{16}O/^{18}O$. For example, they could arise from typical RCB-like mass-ratio mergers but with a smaller total mass, smaller convective envelope or a smaller hydrogen content than typical. Another interesting possibility is that some dLHdC stars undergo a short-lived, dust forming phase. During this phase, these stars would be observed as dust-forming RCB-like stars with low $^{16}O/^{18}O$ – similar to the five RCB stars mentioned above. This scenario does not contradict the observation that dLHdC stars do not show significant excesses in the mid-IR WISE bands. Tisserand et al. 2022 show that the emission from a circumstellar dust shell ejected from the surface of a star shifts from the mid-IR to longer wavelengths within a few decades. Thus, even if some dLHdC stars experienced dust formation ∼10 years before their WISE observations, they would not show any excesses in the WISE bands. The dust around them would have cooled to <50 K (see Montiel et al. 2018) and would be observable only at very long wavelengths. Only one dLHdC star has been observed at far-infrared (FIR) wavelengths to date – HD 173409 which did not show any FIR excess (Montiel et al. 2018). Far-infrared and sub-mm observations of the newly identified dLHdC stars will help confirm or rule out the presence of a cold dust shell around them.

Finally, we note that four newly discovered dLHdC stars (A166, C526, F75 and F152) show definite signs of dust formation from their mid-IR colors and light curves (see Sect. 4.5 of Tisserand et al. 2022). Of these, A166 is an outlier within the dLHdC population (see Sect. 4.2.1), has RCB-like $^{16}O/^{18}O$ and is likely an RCB star in a low dust-production phase. The three other stars are not outliers, but are too hot to sustain $^{12}C^{16}O$ and $^{12}C^{18}O$ in their photospheres so their $^{16}O/^{18}O$ cannot be constrained. Sub-mm searches for the colder circumstellar medium of these stars can determine whether they have dLHdC-like or RCB-like $^{16}O/^{18}O$ values. Additional studies of such "overlap" stars are necessary to understand the dust-formation connection between dLHdC and RCB stars.

6. Summary and way forward

^{18}O has been key to understanding the origins of the enigmatic dLHdC and RCB stars. The anomalously large ^{18}O abundance in them can be explained by invoking a He-core and a CO-core white dwarf merger model for their formation. Although there were indications that RCB and dLHdC stars have different values of $^{16}O/^{18}O$, the limited sample of dLHdC stars prevented a quantitative comparison. In this paper, we have utilized the revolutionary discovery of 27 new Galactic dLHdC stars to revisit this question.

We analyzed NIR spectra of 24 dLHdC stars together with unpublished spectra of 49 RCB stars. Owing to the several free parameters and assumptions in our fitting methodology, we obtained wide range estimates of the $^{16}O/^{18}O$ ratios for 7 dLHdC and 33 RCB stars whose spectra contain the $^{12}C^{16}O$ and/or $^{12}C^{18}O$ bands. We find that six of the seven dLHdC stars have $^{16}O/^{18}O < 0.5$, while 28 of the 33 RCB stars have $^{16}O/^{18}O > 1$. Thus, the wide range estimates on the $^{16}O/^{18}O$ ratios (although more uncertain in the coolest RCBs) obtained from the medium resolution spectra analyzed here suggest that most dLHdC stars have lower $^{16}O/^{18}O$ than most RCB stars. If corroborated by future high resolution spectroscopic observations, this will be the first established chemical difference between the two classes of HdC stars. It remains to be seen if and how the lower $^{16}O/^{18}O$ can be related to the lack of dust formation in dLHdC stars.

The different oxygen isotope ratios suggest that there is no evolutionary link between the class of dLHdC and RCB stars. Instead, this observation is consistent with the picture that dLHdC and RCB stars are formed from merging white dwarfs with distinct masses, mass ratios and compositions. Further theoretical studies are required to accurately determine the properties of white dwarfs that merge to form dLHdC versus RCB stars. A small number of RCB stars have uncharacteristically low, dLHdC-like $^{16}O/^{18}O$ values. This could be a consequence of multiple white dwarf properties that can affect the value of $^{16}O/^{18}O$ in the merger product, or can be explained by a short-lived dust formation phase in dLHdC stars. Theoretical models will test the former scenario, while FIR and sub-mm observations will confirm or rule out the latter. Further investigations of these "overlap" stars will shed light on the dLHdC-RCB dust formation mystery.

Future higher resolution NIR spectroscopy of the newly discovered dLHdC stars with CO bands will allow accurate determinations of their $^{16}O/^{18}O$ ratios and will help validate the results presented here. High resolution optical spectroscopy should allow the determination of accurate fluorine abundances in them. As fluorine is also a signature of a white dwarf merger (Pandey et al. 2007), these observations will help determine the properties of progenitors of the hot dLHdC stars that do not show CO overtone bands. High resolution spectroscopy also will potentially identify additional chemical differences between dLHdC and RCB stars (e.g., between their H and N abundances as indicated in Tisserand et al. 2022). and shed further light on their progenitor white dwarf populations.

Acknowledgements. We thank the anonymous referee for helpful comments that improved the quality of this paper. We thank Bradley Munson for useful comments and discussions. PT acknowledges financial support from "Programme National de Physique Stellaire" (PNPS) of CNRS/INSU, France. MMK acknowledges the Heising-Simons foundation for support via a Scialog fellowship of the Research Corporation. MMK acknowledges generous support from the David and Lucille Packard Foundation. SA acknowledges support from the GROWTH PIRE grant 1545949. GC and CC are grateful for support from National Science Foundation Award 1814967. This research is based in part on observations for programs GS-2005B-Q-20, GN-2011A-Q-112, GS-2015B-FT-1 and GS-2016B-FT-6 obtained at the international Gemini Observatory, a program of NSF's NOIRLab, which is managed by the Association of Universities for Research in Astronomy (AURA) under a cooperative agreement with the National Science Foundation. on behalf of the Gemini Observatory partnership: the National Science Foundation (United States), National Research Council (Canada), Agencia Nacional de Investigación y Desarrollo (Chile), Ministerio de Ciencia, Tecnología e Innovación (Argentina), Ministério da Ciência, Tecnologia, Inovações e Comunicações (Brazil), and Korea Astronomy and Space Science Institute (Republic of Korea).

References

Alvarez, R., & Plez, B. 1998, A&A, 330, 1109
Asplund, M., Gustafsson, B., Lambert, D. L., & Rao, N. K. 2000, A&A, 353, 287
Bell, R. A., Eriksson, K., Gustafsson, B., & Nordlund, A. 1976, A&AS, 23, 37
Clayton, G. C. 1996, PASP, 108, 225
Clayton, G. C. 2012, J. Am. Assoc. Variable Star Obs., 40, 539
Clayton, G. C., Geballe, T. R., & Bianchi, L. 2003, ApJ, 595, 412
Clayton, G. C., Herwig, F., Geballe, T. R., et al. 2005, ApJ, 623, L141
Clayton, G. C., Geballe, T. R., Herwig, F., Fryer, C., & Asplund, M. 2007, ApJ, 662, 1220
Clayton, G. C., Sugerman, B. E. K., Stanford, S. A., et al. 2011, ApJ, 743, 44
Crawford, C. L., Clayton, G. C., Munson, B., Chatzopoulos, E., & Frank, J. 2020, MNRAS, 498, 2912
Cushing, M. C., Vacca, W. D., & Rayner, J. T. 2004, PASP, 116, 362
Driebe, T., Schoenberner, D., Bloecker, T., & Herwig, F. 1998, A&A, 339, 123
Eikenberry, S. S., Elston, R., Raines, S. N., et al. 2004, SPIE Conf. Ser., 5492, 1196
Elias, J. H., Rodgers, B., Joyce, R. R., et al. 2006, in SPIE Conf. Ser., 6269, 626914
Feast, M. W. 1996, ASP Conf. Ser., 96, 3
Fryer, C. L., & Diehl, S. 2008, ASP Conf. Ser., 391, 335
García-Hernández, D. A., Hinkle, K. H., Lambert, D. L., & Eriksson, K. 2009, ApJ, 696, 1733
García-Hernández, D. A., Lambert, D. L., Kameswara Rao, N., Hinkle, K. H., & Eriksson, K. 2010, ApJ, 714, 144
Geballe, T. R., Rao, N. K., & Clayton, G. C. 2009, ApJ, 698, 735
Goorvitch, D. 1994, ApJS, 95, 535
Goswami, A., Karinkuzhi, D., & Shantikumar, N. S. 2010, ApJ, 723, L238
Gustafsson, B., Bell, R. A., Eriksson, K., & Nordlund, A. 1975, A&A, 42, 407
Gustafsson, B., Edvardsson, B., Eriksson, K., et al. 2008, A&A, 486, 951
Hansen, C. J., Kawaler, S. D., & Trimble, V. 2004, Stellar Energy Sources (New York: Springer), 271
Hedrosa, R. P., Abia, C., Busso, M., et al. 2013, ApJ, 768, L11
Herter, T. L., Henderson, C. P., Wilson, J. C., et al. 2008, Proc. SPIE, 7014, 70140X
Iben, I., J., & Tutukov, A. V. 1984, ApJS, 54, 335
Jeffery, C. S., Karakas, A. I., & Saio, H. 2011, MNRAS, 414, 3599
Karambelkar, V. R., Kasliwal, M. M., Tisserand, P., et al. 2021, ApJ, 910, 132
Lambert, D. L., & Rao, N. K. 1994, J. Astrophys. Astron., 15, 47
Lauer, A., Chatzopoulos, E., Clayton, G. C., Frank, J., & Marcello, D. C. 2019, MNRAS, 488, 438
Montiel, E. J., Clayton, G. C., Sugerman, B. E. K., et al. 2018, AJ, 156, 148
Munson, B., Chatzopoulos, E., Frank, J., et al. 2021, ApJ, 911, 103
Pandey, G., Lambert, D. L., & Kameswara Rao, N. 2007, ArXiv e-prints [arXiv:0712.3971]
Plez, B. 2008, Phys. Scripta, Vol. T, 133, 014003
Ramsay Howat, S. K., Todd, S., Leggett, S., et al. 2004, SPIE Conf. Ser., 5492, 1160
Rayner, J. T., Toomey, D. W., Onaka, P. M., et al. 2003, PASP, 115, 362
Saio, H., & Jeffery, C. S. 2002, MNRAS, 333, 121
Staff, J. E., Menon, A., Herwig, F., et al. 2012, ApJ, 757, 76
Staff, J. E., Wiggins, B., Marcello, D., et al. 2018, ApJ, 862, 74
Tisserand, P. 2012, A&A, 539, A51
Tisserand, P., Clayton, G. C., Welch, D. L., et al. 2013, A&A, 551, A77
Tisserand, P., Clayton, G. C., Bessell, M. S., et al. 2020, A&A, 635, A14
Tisserand, P., Crawford, C. L., Clayton, G. C., et al. 2022, A&A, 667, A83
Vacca, W. D., Cushing, M. C., & Rayner, J. T. 2003, PASP, 115, 389
Warner, B. 1967, MNRAS, 137, 119
Webbink, R. F. 1984, ApJ, 277, 355
Yurchenko, S. N., Szabó, I., Pyatenko, E., & Tennyson, J. 2018, MNRAS, 480, 3397
Zhang, J., Wang, X., Mazzali, P. A., et al. 2014, ApJ, 797, 5